

Lawrence Berkeley National Laboratory

Recent Work

Title

ACTIVATION ENERGIES FOR THE DISSOCIATION OF DIATOMIC MOLECULES CALCULATED FROM MOLECULAR PROPERTIES

Permalink

<https://escholarship.org/uc/item/8sc7955p>

Authors

Johnston, Harold.

Birks, John.

Publication Date

1971

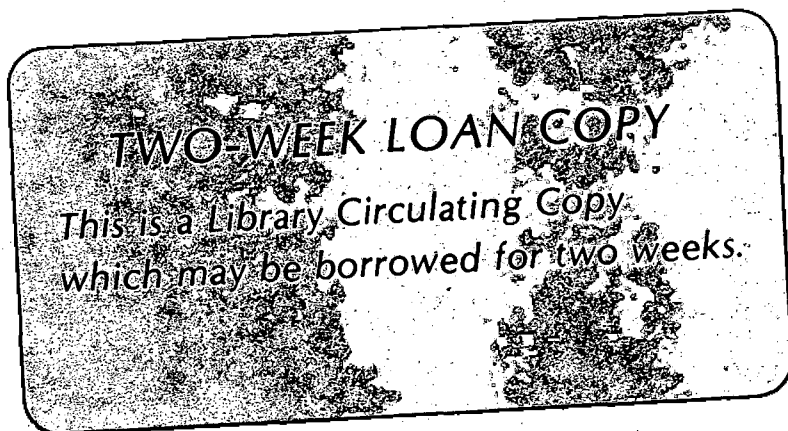
ACTIVATION ENERGIES FOR THE DISSOCIATION OF
DIATOMIC MOLECULES CALCULATED FROM
MOLECULAR PROPERTIES

Harold Johnston and John Birks

January 1971

AEC Contract No. W-7405-eng-48

JUL 9 1987



LAWRENCE RADIATION LABORATORY
UNIVERSITY of CALIFORNIA BERKELEY

DISCLAIMER

This document was prepared as an account of work sponsored by the United States Government. While this document is believed to contain correct information, neither the United States Government nor any agency thereof, nor the Regents of the University of California, nor any of their employees, makes any warranty, express or implied, or assumes any legal responsibility for the accuracy, completeness, or usefulness of any information, apparatus, product, or process disclosed, or represents that its use would not infringe privately owned rights. Reference herein to any specific commercial product, process, or service by its trade name, trademark, manufacturer, or otherwise, does not necessarily constitute or imply its endorsement, recommendation, or favoring by the United States Government or any agency thereof, or the Regents of the University of California. The views and opinions of authors expressed herein do not necessarily state or reflect those of the United States Government or any agency thereof or the Regents of the University of California.

ACTIVATION ENERGIES FOR THE DISSOCIATION OF
DIATOMIC MOLECULES CALCULATED FROM MOLECULAR PROPERTIES

Harold Johnston and John Birks

Inorganic Materials Research Division, Lawrence Radiation Laboratory
Department of Chemistry, University of California, Berkeley, California

ABSTRACT

Rate constants and activation energies for the thermal dissociation of H_2 , N_2 , O_2 , F_2 , Cl_2 , Br_2 , and I_2 are reviewed and summarized. The observed activation energies in all cases are substantially below the bond dissociation energies. Models are set up in terms of energy-transfer processes between the vibrational states of the reactant, and pertinent constants are evaluated from observed spectroscopic parameters, transport properties, and vibrational relaxation times. Non-equilibrium distributions over vibrational states are calculated. The "ladder climbing" model with dissociation occurring only from the top vibrational state gives an incorrect trend of activation energies with temperature. Regardless of the details, each model that permits dissociation from all vibrational states correctly predicts a large decrease in activation energy as temperature increases. At high temperatures, the reaction seriously depletes upper vibrational states, and this decrease in number of states that react causes the rate constant to increase with temperature less rapidly than expected. Thus the activation energy, which is merely a measure of how the rate constant changes with temperature, is lower than the bond dissociation energy.

A. Introduction

The dissociation of a homonuclear diatomic molecule X_2 in a "heat bath" of an inert monatomic gas M appears to be a relatively simple chemical process



In recent years extensive experimental data for H_2 , N_2 , O_2 , F_2 , Cl_2 , Br_2 , and I_2 in Ar and other noble gases have been obtained, Table 1, mostly by use of shock tubes. Rate constants \underline{k}

$$\underline{k} = - \frac{1}{[M]} \frac{d \ln [X_2]}{dt} \quad (2)$$

have been observed over a wide range of temperature, and Arrhenius activation energies have been evaluated

$$\underline{E} = -R \frac{d \ln \underline{k}}{d(1/T)} \quad (3)$$

An interesting feature of the data is that in each case the activation energy is substantially less than the bond dissociation energy, \underline{D}_0° . A number of authors¹⁻¹³ have discussed this phenomenon, and the consensus is that it is a result of a non-equilibrium distribution of reactant molecules over excited vibrational states when reaction occurs. In this article, we review the experimental data for all seven homonuclear diatomic molecules listed above, and we attempt to set up the simplest theory that, without adjustable parameters, gives approximately correct values for the rate constants \underline{k} and that gives an explanation for the "low" activation energies. This "simplest" theory uses the empirical spectroscopic properties

of the reactant, the empirical transport properties of the reactant and catalyst M, and the empirical vibrational relaxation probability $\frac{P}{10}$ for the diatomic molecule.

A firmly entrenched model in many chemists' minds is that the "activation energy" represents a "barrier" between reactants and products, and thus there is a serious conceptual problem in having the observed activation energy be far less than the endothermicity of the reaction. However, this viewpoint puts the pictorial model (barrier height) ahead of the defining relation, Eq.(3); for, after all, the "activation energy" is just a name for how the rate constant k changes with temperature. If the rate constant, for some reason, increases with temperature less rapidly than expected, then the activation energy will be less than expected. If one expects the activation energy to be at least the endothermicity of the reaction and if the rate increases with temperature ~~more~~ ^{less} ~~slowly~~ ^{rapidly} than expected because excited vibrational states of the molecules are depleted below the equilibrium value, then the activation energy, Eq.(3), will be less than the endothermicity. This effect is a particularly large one for the dissociation of diatomic molecules.

A purely formal "explanation" for low activation energies is sometimes given, as follows. If the rate constant for dissociation of a diatomic molecule depends on temperature as

$$k = C T^m \exp(-D_0/RT) \quad (4)$$

then application of Eq.(3) gives the result that the activation energy is

$$\underline{E} = \underline{D}_0^\circ + \underline{m} R \underline{T} \quad (5)$$

where \underline{T} is the average temperature over the range of observation. If \underline{m} is negative, then the activation energy \underline{E} is less than the dissociation energy \underline{D}_0° . If \underline{m} is regarded merely as an empirical parameter, then the invocation of Eqs.(4) and (5) is not an explanation at all, but only another description of the phenomenon. If one adopts a model for the reaction process and assumes that reactants have an equilibrium distribution over vibrational states, then \underline{m} may be evaluated, and it is typically in the range of ± 0.5 (see Section E below). In many cases, the departure of activation energy from dissociation energy far exceeds what can be expected from this effect, confirming the expectation that the low activation energies are a result of non-equilibrium over vibrational states.

B. Experimental Data

The experimental data have been reviewed recently by Troe and Wagner,¹⁴ and our Table I is taken largely from their Table I. In our Table I we give the reactant A, the foreign gas M, the temperature range, the observed activation energy \underline{E} (Eq.3), the parameter \underline{m} (Eq.5), the dissociation energy \underline{D}_0° , and references for experimental studies of the dissociation of homonuclear diatomic molecules.¹⁵⁻⁴⁶ It is readily seen that observed activation energies are far less than bond dissociation energies, and the empirical parameter \underline{m} is always negative, varying from -0.4 to -4.0.

Spectroscopic data, vibrational relaxation times, and hard-spheres collision cross sections^(Table II) were obtained from reference books and certain articles.⁴⁷⁻⁵³ Some articles⁵⁴⁻⁵⁷ have appeared with kinetic data since Troe and Wagner's review. Wherever possible we have prepared tables of rate constants as a function of temperature for comparison with our calculated rate constants. Unfortunately, it is now rare for journals to publish data in this form; rather data appear as mathematical functions, parameters of the Arrhenius equation

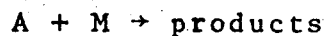
$$k = A \exp(-E/RT) \quad (6)$$

parameters in Eq.(4), or as points on a small figure. Especially for H₂, data are lost in this way, and only line segments of average rate constants^{over} temperature intervals are available for the reinterpretation of data. Wherever possible, we have used tabulated data or data that we have read from figures for detailed comparisons with the models we use.

C. General Molecular Model

The purpose of this paper is to find the simplest possible molecular model that correctly indicates the low activation energies and that utilizes no adjustable parameters. First, we present a general mechanism in terms of vibrational states of the reactant; and next, we set up four specific models for energy-transfer and dissociative processes. The predictions of these models are then compared with experiment.

The chemical reaction of Eq.(1) is abbreviated to read



The individual vibrational states $A_{\underline{i}}$ of the reactant are identified (omission of explicit mention of rotational and translational states implies that the reactant effectively has an equilibrium distribution over such states, and the collision constants later defined include the effect of the equilibrium range of such states). We define three different inelastic collision processes: (1) The rate of activation of A from initial state \underline{i} to final state \underline{j} upon collision with M is

$$R_{\underline{ij}}(\text{up}) = a_{\underline{ij}} [A_{\underline{i}}] [M] \quad (7)$$

(2) The rate of de-activation of A from initial state \underline{i} to final state \underline{j} is

$$R_{\underline{ij}}(\text{down}) = b_{\underline{ij}} [A_{\underline{i}}] [M] \quad (8)$$

(3) The rate of dissociation of A from state \underline{i} to the continuum of free atoms is

$$R_{\underline{ic}} = c_{\underline{i}} [A_{\underline{i}}] [M] \quad (9)$$

The rate of the chemical reaction is then

$$R = - \frac{d[A]}{dt} = \sum_{\underline{i}=0}^{\underline{t}} c_{\underline{i}} [A_{\underline{i}}] [M] \quad (10)$$

where \underline{t} is the "top" bound state of the diatomic molecule A.

The total number of reactant molecules is the sum over all vibrational states

$$[A] = \sum_{\underline{i}} [A_{\underline{i}}] \quad (11)$$

If Eq.(10) is multiplied by $[A]/\sum [A_{\underline{i}}]$ and terms are rearranged, we obtain

$$R = [M][A] \sum_{\underline{i}} c_{\underline{i}} \frac{X_{\underline{i}}}{\sum_{\underline{i}} X_{\underline{i}}} \quad (12)$$

where \underline{X}_i is the mole fraction of molecules in state \underline{i}

$$\underline{X}_i = [A_i]/[A] \quad (13)$$

and the rate constant

$$\underline{k} = \text{Rate}/[M][A] \quad (14)$$

is expressed as

$$\underline{k} = \sum_i c_i \underline{X}_i \quad (15)$$

This general model is illustrated for a truncated harmonic oscillator in Figure 1 and for a Morse oscillator in Figure 2.

For an equilibrium distribution over vibrational states, the mole fraction in state \underline{i} is simply

$$(\underline{X}_i)_{\text{eq}} = \frac{\exp(-\epsilon_i/kT)}{f_v} \quad (16)$$

where ϵ_i is the vibrational energy relative to the zero point level, k is Boltzmann's constant, and f_v is the vibrational partition function. During chemical reaction one does not have an equilibrium distribution over vibrational states, and the mole fractions \underline{X}_i are not easily evaluated. To obtain the actual distribution over vibrational states, one needs to solve the simultaneous rate equations

$$\begin{aligned} \frac{d[A_i]}{dt} = & [M] \sum_{j=0}^{i-1} a_{ji} [A_j] + [M] \sum_{j=i+1}^t b_{ji} [A_j] \\ & - [M][A_i] \left(\sum_{j=0}^{i-1} b_{ij} + \sum_{j=i+1}^t a_{ij} + c_i \right) \end{aligned} \quad (17)$$

with one such equation for each state i from zero to t . It has been shown by detailed computations,¹² that after an extremely short induction period the relative concentrations $[A_i]/[A]$ assume a steady-state distribution, that is, these ratios do not change with time even though the reactant as a whole is rapidly disappearing and each state i decreases accordingly. Thus, as an excellent approximation

$$\frac{d([A_i]/[A])}{dt} \approx 0 \tag{18}$$

$$= \frac{1}{[A]} \frac{d[A_i]}{dt} - \frac{[A_i]}{[A]} \frac{d[A]}{dt} \tag{19}$$

Upon substitution of Eqs. (10) and (17) into Eq. (19), we obtain an expression suitable for evaluating the steady-state concentration of A_i by a method of successive approximations

$$\sum X_i = \frac{\sum_{j=0}^{i-1} a_{ji} X_j + \sum_{j=i+1}^t b_{ji} X_j}{c_i + \sum_{j=0}^{i-1} b_{ij} + \sum_{j=i+1}^t a_{ij} - \sum_{i=0}^t c_i X_i} \tag{20}$$

If one has a set of rate constants a_{ij} , b_{ji} , and c_i , one takes as the zero approximation the equilibrium mole fractions, Eq. (16), to find a first approximation to the set of non-equilibrium mole fractions, X_i ($i=0,1,2,\dots,t$). This first approximation is then substituted into the right hand side of Eq. (20) to find the second approximation to X_i , and the process can be repeated to any desired degree of convergence.

Microscopic reversibility gives a general relation between rate constants for activation and deactivation of diatomic molecules

$$\frac{a_{ij}}{b_{ji}} = \exp[-(\epsilon_j - \epsilon_i)/kT] \quad (21)$$

The remaining problem is to set up models for the evaluation of the detailed rate constants a, b, and c.

D. Four Specific Models

I. Ladder Climbing model with truncated harmonic oscillator.

This model has been used several times in the past. It uses the harmonic-oscillator conditions on light absorption or emission as restrictions on energy transfer such that activation and deactivation occur only between adjacent states

$$a_{ij} = b_{ij} = 0 \text{ for } j \neq i \pm 1 \quad (22)$$

With this restriction, we use the simplified nomenclature

$$a_i = a_{i,i+1}; b_i = b_{i,i-1} \quad (23)$$

A further property of harmonic-oscillator spectroscopy is used to evaluate the deactivation rate constant at any level in terms of the deactivation constant between the two lowest levels

$$b_i = i b_1 \quad (24)$$

From microscopic reversibility, Eq.(21), and from Eq.(24), we obtain a general expression for the activation rate constants

$$a_i = (i+1)b_1 \exp(-h\nu/kT) \quad (25)$$

where h is Planck's constant and ν is the harmonic oscillator vibration frequency. The name "ladder climbing model" implies that the molecule dissociates only from the top vibrational level, t:

$$c_i = 0 \text{ for } i < t \quad (26)$$

The specific assumption made here is that from the top rung, the molecule dissociates upon every sufficiently energetic collision

$$\underline{c}_t = \underline{Z} \exp[-(D_o^\circ - \underline{\epsilon}_t)/kT] \quad (27)$$

where \underline{Z} is the rate constant for a hard-spheres collision

$$\underline{Z} = \pi \sigma^2 (8kT/\pi\mu)^{1/2} \quad (28)$$

σ is the hard-spheres collision diameter (evaluated from viscosity, for example), and μ is the reduced mass between A and M.

The evaluation of the vibrational relaxation constant \underline{b}_{10} or \underline{b}_1 is thoroughly explained by recent books in this field.^{47,48} We need this constant as a function of temperature, and the most convenient form is the table and interpolation formula by Millikan and White.⁴⁹ In this way we find \underline{b}_1 for all diatomic molecules at all temperatures of interest, except H_2 , which is not included in Millikan and White's list. To obtain the value for H_2 in Ar, we use Mahan's⁵⁰ recently proposed theoretical model. The agreement of this theoretical function with the meager experimental data is shown by Fig. 3. Molecular properties needed to evaluate the collision constant ~~is~~^{are} given in Table II.

II. Truncated Harmonic Oscillator (Fig. 1)

This model is the same as I except that we accept the possibility of dissociation of the reactant from any vibrational state \underline{i} , instead of just the top state \underline{t} . From a given state \underline{i} , activation can occur to only one final state $\underline{i}+1$ with an energy jump of $\underline{h\nu}$; but dissociation can occur into the con-

tinuum of states with an energy jump of $(D_0^\circ - \epsilon_i)$ or more. Except for the greater jump in energy, the transition to the continuum should be more probable than transition to the single state $i+1$ because of the greater density of final states. It is assumed that the ratio of dissociation to activation is

$$\frac{c_i}{a_i} = \beta \frac{\exp[-(D_0^\circ - \epsilon_i)/kT]}{\exp[-h\nu/kT]} \quad (29)$$

where $\beta > 1$ and is the same for all states i . The value of β can be found from the expression for c_i , Eq.(27). With β evaluated from Eq.(27) and with a_i obtained from Eq.(25), we have a general expression for the dissociation rate constants

$$c_i = \frac{i+1}{t+1} Z \exp[-(D_0^\circ - \epsilon_i)/kT] \quad (30)$$

For this model a_i and b_i are the same as for model I, respectively, Eq.(25) and Eq.(24).

It is sometimes argued that a model such as this one is very poor, because it can be shown that large jumps in energy are highly improbable. To be sure, large jumps are improbable as one can see by substitution into Eq.(30), but populations in high quantum states are also improbable. The distribution function for states that react is $c_i X_i$, Eq.(15). The term c_i contains the exponential term $\exp[-(D_0^\circ - \epsilon_i)/kT]$ and the equilibrium mole fraction X_i contains the exponential term $\exp[-\epsilon_i/kT]$, see Eq.(16). The product of the rate constant, Eq.(30), and the equilibrium mole fraction is simply $(Z/f_v)(i+1)/(t+1) \exp[-D_0^\circ/kT]$, which varies only slowly with quantum state i . From this relation it can be seen that at equilibrium all vibrational states contribute approximately the same amount to the decomposition

rate--they differ only by the factor $(i+1)/(t+1)$. There are $t+1$ approximately equal, parallel channels of reaction, some involving low lying reactants making improbable big jumps to dissociation and some involving improbable highly vibrationally excited reactants making small jumps to dissociation. There is no rate determining step nor single "activated complex." These $t+1$ parallel reaction channels constitute the so-called "entropy of activation."

III. Morse oscillator with transitions between adjacent levels.

The vibrational energy levels for the Morse oscillator are

$$\frac{\epsilon_i}{hc} = (i+\frac{1}{2})\omega_e - (i+\frac{1}{2})^2\omega_e x_e \quad (31)$$

where c is the velocity of light, ω is the fundamental frequency in cm^{-1} and x_e is the anharmonicity constant. Both ω_e and x_e are readily evaluated from spectroscopic data.⁵² A convenient formula⁵³ for transition probabilities for the Morse oscillator has been given

$$b_{i+r,i} = b_{ro} \frac{(r+i)!}{r! i!} (1+rx_e) \quad (32)$$

With restriction to nearest-neighbor transitions, all constants can be evaluated in terms of b_1

$$b_i = i b_1 (1+x_e) \quad (33)$$

$$a_i = (i+1)b_1(1+x_e) \exp[-(\epsilon_{i+1} - \epsilon_i)/kT] \quad (34)$$

With this model transitions to the continuum are allowed for all states, and c_i has the same form as for model II, Eq.(30), except that the number of states t is greater for model III than for model II.

IV. Morse oscillator with all transitions allowed (Fig. 3).

Stevens⁴⁸ gives a model for transitions that readily permits all values of deactivation constants b_{ij} to be found:

$$b_{i+r,i} = b_{10} x e^{\frac{r-1}{i! r^2} (i+r)!} \quad (34)$$

From microscopic reversibility, the activation constants a_{ij} are obtained

$$a_{i,i+r} = b_{10} x e^{\frac{r-1}{i! r^2} (i+r)!} \exp[-(D_0^\circ - \epsilon_i)/kT] \quad (35)$$

The rate constants for dissociation from any state are the same as for models II and III.

$$c_i = \frac{(i+1)}{(t+1)} Z \exp[-(D_0^\circ - \epsilon_i)/kT]$$

These constants may be factored into the collision rate constant Z and the transition probability P

$$\begin{aligned} a_{ij} &= Z P_{ij} \\ b_{ij} &= Z P_{ij} \\ c_i &= Z P_{ic} \end{aligned} \quad (36)$$

For H_2 in Ar at 5000°K, the transition probability matrix P_{ij} is given by Table III. The dissociation probability vector P_{ic} is given in the same table. Although this model permits all transitions, large changes in vibrational quantum number are of low probability. It is interesting to note that for quantum levels above the ninth, dissociation to the dense states of the continuum is more probable than deactivation to the small number of low lying vibrational states. Above the eighth state, dissociation

across many quantum states is more probable than activation to the next higher state. The density of final states is an important factor in determining transition rates.

For the four models, we can evaluate all values of the energy-transfer functions a_{ij} and b_{ij} and the dissociation constants c_i from molecular properties obtained by separate experiments: b_{10} , vibrational relaxation; ω and x_e , Raman spectroscopy; Z , viscosity or second virial coefficients. With these constants we evaluate the vibrational distribution function by successive approximations from Eq.(20), the rate constants from Eq.(15), and the activation energy from Eq.(3). In the next sections we test the predictions of E and k by the four models, first for the hypothetical situation of reactant with an equilibrium distribution over vibrational states and next for non-equilibrium, steady-state, relative distribution functions.

E. Model Predictions if Reactants Have Equilibrium Distribution Function

For rate expression, we go back to Eq.(10), $\sum_i c_i [A_i] [M]$. Using Eq.(16) for the equilibrium concentration of reactant in the vibrational state i , we obtain

$$R_{eq} = [M][A_0] \sum_i \frac{c_i}{\omega_i} e^{-\epsilon_i/kT} \quad (37)$$

The total concentration of reactant is the sum over all states

$$\begin{aligned} [A] &= \sum_i [A_i] = [A_0] \sum_i e^{-\epsilon_i/kT} \\ &= [A_0] f_v \end{aligned} \quad (38)$$

where f_v is the vibrational partition function. Thus the rate expression is

$$R_{eq} = [M][A] \frac{1}{f_v} \sum_i c_i e^{-\epsilon_i/kT} \quad (39)$$

and the rate constant is

$$k_{eq} = \frac{1}{f_v} \sum_i c_i e^{-\epsilon_i/kT} \quad (40)$$

For model I, there is only one term in the sum, since c_i is assumed to be zero for all states except the top one t

$$\begin{aligned} k_{eq}^I &= \frac{1}{f_v} Z \exp[-(D_0^o - \epsilon_t)/kT] e^{-\epsilon_t/kT} \quad \text{exp}[-\epsilon_t/kT] \\ &= (Z/f_v) \exp[-D_0^o/kT] \end{aligned} \quad (41)$$

For models II, III, and IV the rate constant expression is given by

$$\begin{aligned} k_{eq} &= \frac{Z}{f_v} \sum_i \frac{i+1}{t+1} \exp[-(D_0^o - \epsilon_i)/kT] \exp[-\epsilon_i/kT] \\ &= (Z/f_v) \exp[-D_0^o/kT] \sum_{i=0}^t \frac{i+1}{t+1} \\ &= (Z/f_v) \exp[-D_0^o/kT] \left(\frac{t+2}{2}\right) \end{aligned} \quad (42)$$

Thus the temperature dependence of all four models is the same if there is an equilibrium distribution over vibrational states

$$E_{eq} = D_0^o - R \frac{d \ln Z}{d(1/T)} + R \frac{d \ln f_v}{d(1/T)} \quad (43)$$

For the harmonic oscillators, models I and II, the vibrational partition function is approximately $(1 - e^{-h\nu/kT})^{-1}$, its temperature derivative in Eq. (43) varies between 0 at low temperature and RT at high temperature. If the collision rate constant varies as $T^{-1/2}$, Eq. (28), its contribution to the activation

energy is $\frac{1}{2} RT$. Thus these two models predict

$$\underbrace{D_0^\circ - \frac{1}{2} RT}_{\text{High T limit}} \leq E_{\text{eq}} \leq \underbrace{D_0^\circ + \frac{1}{2} RT}_{\text{Low T limit}} \quad (44)$$

The observed activation energies in Table I differ from D_0° substantially more than the limits given by Eq.(44). Thus these models are inadequate to explain the observed activation energies if the vibrational states have an equilibrium distribution. Similar conclusions apply to models III and IV if the quantities are evaluated numerically.

F. Calculated Activation Energies and Rate Constants with Non-Equilibrium Distribution Function

Hydrogen--By use of the values of the transition constants for activation, deactivation, and dissociation, rate constants and activation energies for the dissociation of H_2 in a heat bath of Ar were calculated each 400° between 1000° and $7000^\circ K$. For each of the four models, the results are given in Table IV. Similar results for F_2 between 500 and $5000^\circ K$ are included in Table IV. It is readily apparent that the ladder-climbing model gives activation energies that vary with temperature in a manner quite different from that observed. At low temperatures, this model greatly underestimates the rate. At high temperatures where vibrational energy transfer becomes fast, the rate constants are less than those calculated by the other models, but the difference is much less than that found at low temperatures. This partial "catching-up" at high temperatures causes the rate to increase faster than expected at high temperatures, and the activation ^{energy} greatly exceeds the dissociation energy.

The other three models show activation energies that decrease with temperature, in the same general sense as that observed.

The calculated and observed rate constants k_A for H_2 are compared in Figure 4. Calculated curves are given for model I and model IV (models II and III are too similar to model IV to make those plots worthwhile). The experimental data are not given as individual points but as line segments covering the observed temperature range and the reported Arrhenius parameters (this is the only form in which most of these data are available). The experimental data show substantial disagreement between different investigators. Even so, the rate constants for model I ~~is~~ ^{are} well below the experimental data, and those for models II, III, and IV are in reasonably good agreement with the data. On the basis of these results, model I is dropped from further consideration.

Fluorine--For fluorine, data are available for b_{10} as a function of temperature⁴⁹ (unlike H_2 where the function was calculated⁵⁰). Fluorine is relatively insensitive to trace impurities, whereas H_2 and Cl_2 are susceptible to traces of O_2 (H_2 being attacked by O or HO ; Cl_2 dissociating by way of ClO and ClO ⁵⁸). Thus, fluorine was chosen for the most intensive calculations, and in particular for comparisons of model II and model IV.

equilibrium and non-equilibrium
The distribution of F_2 over vibrational states

are given in Table V in terms of the mole fraction X_{iA} of the full Morse calculation (model IV). The logarithm of mole fraction X_{iA} is given as a function of vibrational energy for 500, 1000, and 2500°K. At 500°K, the

steady-state distribution is very close to the equilibrium distribution up to the 17th quantum state, and then it rapidly falls off at higher states. At 1000°K, the fall-off begins at about state 11. At 2500°K there is serious depletion of excited vibrational states above the third or fourth level. Table V also gives the dissociation rate constants c_i as a function of quantum state and temperature. At very high quantum numbers, the constant c_i differs only slightly between 500, 1000, and 2500°K. At low quantum numbers there is a great spread with temperature in c_i at a given state i . The relative "distribution function for molecules that react" is given by the products of mole fractions $\frac{x_i}{\sum x_i}$ and dissociation constant c_i , and these are given for three temperatures as Figure 5. At 500°K, the contribution to reaction is almost uniform from states 2 to 20, with a slight drop off at low quantum numbers (see Eq.30) and a large drop off at high quantum numbers from non-equilibrium. At 1000°K the reacting states are equally important from about 2 to 15. At 2500°K the states that react lie largely between 0 and 7, with a fairly fast fall-off above the seventh state. Figure 5 alone explains why the activation energy decreases with increasing temperature: With an equilibrium distribution all 29 states react equally except for the factor $(i+1)/(t+1)$, Eq.(30), and thus there are 29 parallel reaction channels. At 500°K the decomposition reaction has set up a steady-state distribution such that upper states are depleted. The depletion of a given

state 1 is caused both by the rapid loss of 1 states to atoms and by state 1 being skipped as lower states go directly to atoms. From Figure 5, we see that at 500°K there are only about 20 reaction channels; at 1000°K the number is about 15; and at 2500°K the number is about 7. This decrease in "number of states that react" by virtue of the non-equilibrium distribution at high energies causes the rate constant to increase with temperature ^{less rapidly} ~~slower~~ than expected, and thus the activation energy is lower than expected (see Eq.3).

The observed rate constants ^{for F₂} ~~are~~ are shown in Figure 6 with curves calculated by model II and model IV (results for model III are almost identical with model IV). These two models agree fairly well with the data, and they agree so closely with each other that the simpler model II is selected for all further comparisons.

All other cases--By use of the truncated harmonic oscillator model (Fig. 1 and model II), the activation energies as a function of temperature were calculated for all four halogens, and the data are given in Table VI. Similar data for N₂ and O₂ are given in Table VII. The calculated activation energies decrease strongly with temperature in all cases. These calculations were extended to cover the range of observed temperatures for the various cases in Table I. The last column in that table gives activation energies calculated by means of the truncated harmonic oscillator, model II. Within the experimental uncertainty of the data, the calculated activation energies agree very well with those observed.

Observed rate constants for I_2 , Br_2 , Cl_2 , N_2 , and O_2 are plotted in Figure 7A,B,C,D, and E. Two calculated curves are given on each figure, each is based on model II. The upper curve is calculated on the basis of an equilibrium distribution over vibrational states, and the lower curve is based on the actual, non-equilibrium distribution. The data for I_2 , N_2 , and even O_2 are fairly well defined and show adequate agreement between different investigators. In these cases the non-equilibrium curve calculated from model II agrees fairly well with the observed points, and the equilibrium curve lies well above the data. The data for Br_2 and especially Cl_2 show strong disagreements between different investigators (perhaps due to participation of small amounts of O_2 impurities as catalyst via Cl_{100} and Cl_{10}^{58}). The data for Cl_2 and Br_2 show so much experimental error that it is not useful to speak of agreement or non-agreement between calculated and observed rate constants.

The data for O_2 cover a wider range of temperature than any other, up to $18,000^\circ K$. The calculated non-equilibrium curve shows an increase in activation energy at extremely high temperatures (all other cases show this same effect at temperatures well above the range of observations). The experimental data for O_2 do not show this effect, but it would be difficult to extract it from the data since it appears only above $10,000^\circ K$. The explanation of this effect can be seen by examination and extension of the distribution function for molecules that react in Fig. 5. At the highest temperature shown there, the states that react are the bottom 6 or 7. At even higher temperatures it may be expected that this function will be narrowed to the

lowest one or two states. Then the only reaction is the strong collision channel from the ground state to the continuum, for which single process there is an energy barrier of D_0° . The rate can no longer abstain from increasing "as expected" because the number of states that react cannot shrink below one (This ultimate increase of activation energy at very high temperature might be observed with F_2).

F. The Reverse Reaction

These calculations all refer to the forward reaction or dissociation of the diatomic molecule, Eq.(1), and no account has been given to the reverse process or the recombination reaction. As atoms accumulate and recombination occurs, the population of highly excited vibrational states will surely change in the direction of increased occupancy. As illustrated by Table III, there are many upper vibrational states for which a collision is more likely to give re-dissociation than de-activation. This fact is of importance to the theory of recombination of atoms. Many theories of recombination regard that process as complete when the atom pair is deactivated below the dissociation limit, D_0° . However, the highly excited vibrational states of X_2 are, in effect, closer to products than to reactant. The negative activation energy for atom recombination arises, in part, from the redissociation of highly excited X_2 , an effect that increases with increasing temperature, Figure

G. Summary

In general, the observed activation energy for the dissociation of diatomic molecules is substantially less than the bond dissociation energy, and it decreases with increasing temperature. This effect cannot be explained by a ladder-climbing model of the reaction process with dissociation occurring only from the top vibrational level, even with allowance for a non-equilibrium distribution over vibrational states. This effect is readily explained by several models that allow dissociation to occur from any and all vibrational states and with allowance for non-equilibrium distribution over vibrational states. Three such models were set up that permitted the calculation of dissociation rate constants from separately determined vibrational relaxation times, vibrational frequency, and hard-spheres collision cross section--with no adjustable parameters. The non-equilibrium versions of these models give satisfactory predictions of rate constants and an excellent quantitative account of the observed low activation energies. These calculations indicate that diatomic molecules dissociate from all vibrational states, even though vibrational-vibrational transitions occur primarily between near neighbors.

This work was done under the auspices of the U. S. Atomic Energy Commission.

References

1. O.K. Rice, J. Chem. Phys. 9, 259 (1941); 21, 750 (1953).
2. G. Careri, J. Chem. Phys. 21, 749 (1953).
3. S.K. Kim, J. Chem. Phys. 28, 1057 (1958).
4. K.E. Shuler, J. Chem. Phys. 31, 1375 (1959).
5. E.E. Nikitin and N.D. Sokolov, J. Chem. Phys. 31, 1371 (1959).
6. H.O. Pritchard, J. Phys. Chem. 65, 504 (1961).
7. S.W. Benson and T. Fueno, J. Chem. Phys. 36, 1597 (1962).
8. B. Widom, J. Chem. Phys. 34, 2050 (1961).
9. O.K. Rice, J. Phys. Chem. 67, 6 (1962).
10. P.V. Marrone and C.E. Treanor, J. Phys. Fluids, 6, 1215 (1963).
11. W.G. Valance and E.W. Schlag, J. Chem. Phys. 45, 216, 4280 (1966).
12. D.G. Rush and H.O. Pritchard, International Symposium on Combustion, XI, 13 (1966).
13. V.H. Shui, J.P. Appleton, and J.C. Keck, J. Chem. Phys. 53, 2547 (1970).
14. J. Troe and H.G. Wagner, Ber. Bunsengesellschaft, 71, 930 (1967).
15. C.D. Johnson and D. Britton, J. Phys. Chem. 68, 3032 (1964).
16. R.W. Diesen, J. Chem. Phys. 44, 3662 (1966).
17. D.J. Seery and D. Britton, J. Phys. Chem. 70, 4074 (1966).
18. T.A. Jacobs and R.R. Giedt, J. Chem. Phys. 39, 749 (1963).
19. H. Hiraoka and R. Hardwick, J. Chem. Phys. 36, 1715 (1962).
20. R.W. Diesen and W.J. Felmlee, J. Chem. Phys. 39, 2115 (1963).

21. M. van Thiel, D.J. Seery, and D. Britton, J. Phys. Chem. 69, 834 (1965).
22. R.A. Carabetta and H.B. Palmer, J. Chem. Phys. 46, 1333 (1967).
23. D. Britton, J. Phys. Chem. 64, 742 (1960).
24. D. Britton and N. Davidson, J. Chem. Phys. 25, 810 (1956).
25. H.B. Palmer and D.F. Hornig, J. Chem. Phys. 26, 98 (1957).
26. D. Britton, N. Davidson, W. Gehman, and G. Schott, J. Chem. Phys. 25, 804 (1956).
27. D. Britton, N. Davidson, and G. Schott, Disc. Faraday Soc. 17, 58 (1954).
28. J. Troe and H.Gg. Wagner, Z physik. Chem. N.F. 55, 326 (1967).
29. H.S. Johnston, "Gas Phase Kinetics of Neutral Oxygen Species" National Standard Reference Data Series, National Bureau of Standards, Volume 20 (1968).
30. K.L. Wray, International Symposium on Combustion, X, 523 (1965); J. Chem. Phys. 37, 1254 (1962); 38, 1518 (1963).
31. J.P. Rink, J. Chem. Phys. 36, 572 (1962).
32. J.P. Rink, H. Knight, and R. Duff, J. Chem. Phys. 34, 1942 (1961).
33. O.L. Anderson, United Aircraft Corporation Research Laboratory, Report R-1828-1 (1961).
34. M. Camac and A. Vaughn, J. Chem. Phys. 34, 460 (1961).
35. S.R. Byron, J. Chem. Phys. 30, 1380 (1959).
36. D.L. Matthews, Physics Fluids, 2, 170 (1959).
37. S.A. Losev and N.A. Generalov, Soviet Physics, Doklady, 6, 1081 (1962).

38. N.A. Generalov and S.A. Losev, J. Quant. Spect. Rad. Transfer 6, 101 (1966).
39. E.A. Sutton, J. Chem. Phys. 36, 2923 (1962).
40. R.W. Patch, J. Chem. Phys. 36, 1919 (1962).
41. J.P. Rink, J. Chem. Phys. 36, 262 (1962).
42. A.L. Myerson, H.M. Thompson, and P.J. Joseph, J. Chem. Phys. 42, 3331 (1965); W.S. Watt and A.L. Myerson, 6 Intern. Shock Tube Symposium, Freiburg (1967).
43. W.C. Gardiner and G.B. Kistiakowsky, J. Chem. Phys. 35, 1765 (1961).
44. J.P. Rink, J. Chem. Phys. 36, 1398 (1962).
45. S.R. Byron, J. Chem. Phys. 44, 1378 (1966).
46. B. Cary, Physics Fluids, 8, 26 (1965).
47. T.L. Cottrell and C. McCoubry, "Molecular Energy Transfer in Gases" Butterworths, London (1961), p.77.
48. Brian Stevens, "Collisional Activation in Gases" Pergamon Press, New York (1967), p.39.
49. R.C. Millikan and D.R. White, J. Chem. Phys. 39, 3209 (1963).
50. B.H. Mahan, J. Chem. Phys. 52, 5221 (1970).
51. J.O. Hirschfelder, C.F. Curtiss, and R.B. Bird, "Molecular Theory of Gases and Liquids" Wiley, New York (1954).
52. Gerhard Herzfeld, "Spectra of Diatomic Molecules" Von Nostrand, New York (1950).
53. R.C. Herman and K.L. Shuler, J. Chem. Phys. 16, 373 (1953).
54. R.W. Diesen, J. Phys. Chem. 72, 108 (1968).

55. R.K. Boyd, J.D. Brown, G. Burns, J.H. Lippiatt, J. Chem. Phys. 49, 3822 (1968).
56. R.K. Boyd, G. Burns, T.R. Lawrence, J.H. Lippiatt, J. Chem. Phys. 49, 3804 (1968).
57. J.P. Appleton, M. Steinberg, and D.J. Liquornik, J. Chem. Phys. 48, 599 (1968).
58. H.S. Johnston, E.D. Morris Jr., and Jack Van der Bogaerde, J. Am. Chem. Soc. 91, 7712 (1969).

Table I. Experimental Data on Activation Energies for the Dissociation of Homonuclear Diatomic Molecules.

A	M	T	D_0° kcal	E_{obs} kcal	$\frac{m}{Eq. 5}$	Ref.	$E_{Model}^{calc II}$
F ₂	Ar	1300-1600	37.1	30±4	-2.5	15	31.7
	Ne	1650-2700		24±5	-3.0	16	30.3
	Ar	1300-1600		27.3±2.5	-3.4	17	31.7
	Xe	1300-1600		31.1	-2.1	17	31.7
Cl ₂	Ar	1700-2500	57.0	48.3	-2.1	18	48.4
		1600-2600		50	-1.7	19	49.9
		1700-2600		41±5	-4.0	20	48.6
		1600-2600		45±2	-2.9	21	49.9
		1700-2600		48.3	-2.0	22	48.2
Br ₂	Ar	1300-1900	45.5	41.4	-1.3	23	39.7
		1400-2700		41.4	-1.0	24	38.5
		1200-2200		32.4	-3.8	25	40.3
I ₂	Ar	1000-1600	35.6	29.7	-2.3	26,27	31.6
		850-1650		30.4	-2.1	28	31.9
O ₂	Ar	5000-18000	118.0	110	-0.4	29,30	102.7
		3800-5000		106±5	-1.4	31,32	99.1
		4000-6000		108	-1.0	33	97.5
		3400-7500		108	-1.2	34	97.7
		3000-5000		114	-0.5	35	103.7
	O ₂	3000-5000		98	-2.5	29,36	
		4000-7000		91	-2.5	37	96.4
	2500-4000		108	-1.5	35	108.2	

Table I. Cont'd.

A	M	T	$\frac{D^{\circ}}{\text{kcal}}$	$\frac{E_{\text{obs}}}{\text{kcal}}$	$\frac{m}{\text{Eq. 5}}$	Ref.	$\frac{E_{\text{calc}}}{\text{Model fit}}$
H ₂		3000-6000		109±5	-1.0	32	102.0
		2600-7000		85	-3.7	38	103.3
	Ar	2800-4500	103.3	97	-0.9	39	100.5
		3000-5300		97	-0.8	40	99.6
		2800-5000		97	-0.8	41	100.0
		2150-3650		97.2	-1.0	42	101.9
	Xe	3000-4500		100	-0.4	43	100.5
	H ₂	3000-4500		92	-1.5	43	
D ₂	H	3000-4500		100	-0.4	43	
	Ar	3000-4800	105	97	-1.0	39	
	Ar	3000-4900		97	-1.0	44	
N ₂	Ar	6000-9000	225	218	-0.5	45	195.4
		6000-10000		204	-1.3	46	193.9
	N ₂	6000-9000		218	-0.5	45	195.4
		6000-10000		198	-1.7	46	193.9
	N	6000-9000		203	-1.5	45	

Table II. Molecular Properties Used to Evaluate Vibrational Relaxation Constant $b_1(T)$ and hard-spheres Collision Constant z .

A	M	ω_{e1} cm	$\omega_e X_e$	$\frac{t+1}{\text{no. of states}}$	D_0° kcal mole	ϵ/k $^\circ\text{K}$ of A	$\frac{r_0}{A}$	$\frac{A}{\text{of Ref. 49}}$
H ₂	Ar	4395	126.2	14	103.3	38	2.93	-
H ₂	Ar	4395	0	8	103.3	38	2.93	-
F ₂	F ₂	892	15.3 14.8	29	37.1	112	3.65	65
F ₂	F ₂	892	0	15	37.1	112	3.65	65
Cl ₂	Cl ₂	557	0	36	57.1	257	4.40	58
Br ₂	Br ₂	321	0	50	45.5	520	4.27	48
I ₂	I ₂	213	0	58	35.5	550	4.98	29
N ₂	N ₂	2331	0	33	225	91.5	3.68	220
O ₂	Ar	1554	0	27	118	113	3.43	129
O ₂	O ₂	1554	0	27	118	113	3.43	165
Ref.		52				51	51	49

Table III. Transition Probabilities Per Collision for H₂ With Ar at 5000°K.

$\frac{j}{i}$	0	1	2	3	4	5	6	7	8	9	10	11	12	13
0		.65E-02	.93E-04	.36E-05	.23E-06	.21E-07	.25E-08	.37E-09	.66E-10	.13E-10	.31E-11	.82E-12	.24E-12	.75E-13
1	.20E-02		.13E-01	.28E-03	.14E-04	.12E-05	.13E-06	.18E-07	.30E-08	.59E-09	.13E-09	.34E-10	.98E-11	.31E-11
2	.92E-05	.42E-02		.19E-01	.56E-03	.36E-04	.35E-05	.44E-06	.71E-07	.13E-07	.30E-08	.74E-09	.21E-09	.64E-10
3	.12E-06	.32E-04	.68E-02		.26E-01	.93E-03	.71E-04	.81E-05	.12E-05	.21E-06	.45E-07	.11E-07	.30E-08	.89E-09
4	.30E-08	.62E-06	.74E-04	.98E-02		.32E-01	.14E-02	.12E-03	.16E-04	.27E-05	.53E-06	.12E-06	.33E-07	.96E-08
5	.11E-09	.20E-07	.19E-05	.14E-03	.13E-01		.39E-01	.20E-02	.20E-03	.29E-04	.53E-05	.12E-05	.30E-06	.85E-07
6	.59E-11	.97E-09	.81E-07	.48E-05	.25E-03	.17E-01		.45E-01	.26E-02	.30E-03	.48E-04	.98E-05	.23E-05	.64E-06
7	.41E-12	.64E-10	.49E-08	.25E-06	.10E-04	.40E-03	.21E-01		.52E-01	.34E-02	.43E-03	.76E-04	.17E-04	.44E-05
8	.36E-13	.54E-11	.39E-09	.19E-07	.68E-06	.21E-04	.62E-03	.26E-01		.58E-01	.42E-02	.59E-03	.11E-03	.27E-04
9	.40E-14	.58E-12	.41E-10	.18E-08	.61E-07	.16E-05	.39E-04	.92E-03	.32E-01		.65E-01	.51E-02	.79E-03	.16E-03
10	.55E-15	.77E-13	.52E-11	.23E-09	.71E-08	.17E-06	.36E-05	.68E-04	.13E-02	.38E-01		.71E-01	.62E-02	.10E-0
11	.90E-16	.12E-13	.82E-12	.34E-10	.10E-08	.24E-07	.46E-06	.76E-05	.12E-03	.19E-02	.45E-01		.78E-01	.73E-02
12	.17E-16	.24E-14	.15E-12	.63E-11	.18E-09	.41E-08	.74E-07	.11E-05	.15E-04	.19E-03	.26E-02	.53E-01		.84E-01
13	.40E-17	.54E-15	.35E-13	.14E-11	.39E-10	.85E-09	.15E-07	.21E-06	.27E-05	.30E-04	.31E-03	.36E-02	.61E-01	
P _{ic}	.23E-05	.14E-04	.68E-04	.26E-03	.84E-03	.28E-02	.73E-02	.19E-01	.43E-01	.90E-01	.18	.33	.56	.89

$\frac{P_{ij}}{A_j}$ -- transition probability from vibrational state i to state j .

$\frac{P_{ic}}{A_c}$ -- transition probability from vibrational state i to continuum of dissociated atoms.

Table IV. Dissociation of Hydrogen by Argon. Calculated Activation Energies for Models.

A. Dissociation of Hydrogen by Argon				
T °K	I	II	III	IV
	<u>E, kcal/mole</u>			
1000	99.2	103.9	103.5	103.5
1400	102.0	103.7	103.3	103.0
1800	104.5	103.4	102.8	102.8
2200	106.7	102.9	102.3	102.1
2600	108.4	102.3	101.8	101.5
3000	110.0	101.8	100.8	100.4
3400	111.1	100.8	100.1	99.6
3800	112.2	99.9	99.1	98.6
4200	113.2	99.5	98.6	98.0
4600	113.6	98.5	98.1	97.5
5000	114.0	98.0	97.4	96.7
5400	115.0	98.0	97.0	96.3
5800	115.1	97.5	97.4	96.7
6200	115.4	97.5	97.1	96.4
6600	116.1	98.1	97.6	96.9
7000				

B. Dissociation of Fluorine by Neon				
500	38.5	36.8	36.5	36.5
555	38.7	36.6	36.3	36.3
625	39.0	36.3	36.1	-
714	39.3	35.9	35.6	-
833	39.7	35.3	34.9	34.8
1000	40.3	34.1	33.8	34.7
1250	41.2	32.1	31.9	30.6
1667	42.5	29.8	29.6	29.3
2500	45.4	33.1	32.4	-
5000				

Table V. Mole Fractions in Various Vibrational States and the Dissociation Rate Constant for Vibrational States of Fluorine as a Function of Temperature.

Quantum Number, i	Energy cm^{-1}	500°K			1000°K			2500°K		
		$\log X_{i,eq}$	$\log X_i$	$\log c_i$	$\log X_{i,eq}$	$\log X_i$	$\log c_i$	$\log X_{i,eq}$	$\log X_i$	$\log c_i$
0	442	-0.04	-0.04	-26.92	-0.15	-0.15	-18.72	-0.44	-0.30	-13.71
1	1305	-1.12	-1.12	-25.67	-0.69	-0.69	-18.00	-0.65	-0.59	-13.32
2	2138	-2.16	-2.16	-24.50	-1.21	-1.21	-17.36	-0.85	-0.89	-12.98
3	2941	-3.16	-3.16	-23.40	-1.71	-1.71	-16.76	-1.06	-1.22	-12.69
4	3714	-4.13	-4.13	-22.35	-2.20	-2.20	-16.20	-1.25	-1.56	-12.41
5	4458	-5.06	-5.06	-21.36	-2.67	-2.67	-15.66	-1.43	-1.92	-12.16
6	5173	-5.95	-5.95	-20.41	-3.11	-3.12	-15.16	-1.62	-2.32	-11.92
7	5858	-6.81	-6.81	-19.50	-3.54	-3.56	-14.68	-1.79	-2.75	-11.70
8	6513	-7.62	-7.62	-18.63	-3.95	-3.99	-14.23	-1.95	-3.22	-11.49
9	7138	-8.41	-8.41	-17.81	-3.33	-4.42	-13.79	-2.10	-3.74	-11.30
10	7734	-9.15	-9.15	-17.03	-4.71	-4.87	-13.38	-2.26	-4.32	-11.11
11	8301	-9.86	-9.86	-16.29	-5.06	-5.34	-12.99	-2.39	-4.94	-10.93
12	8838	-10.53	-10.84	-15.58	-5.39	-5.86	-12.63	-2.53	-5.62	-10.77
13	9345	-11.16	-11.18	-14.92	-5.71	-6.46	-12.28	-2.66	-6.35	-10.61
14	9822	-11.76	-11.82	-14.29	-6.01	-7.16	-11.95	-2.77	-7.12	-10.46
15	10270	-12.32	-12.48	-13.71	-6.29	-7.98	-11.65	-2.89	-7.94	-10.32
16	10689	-12.84	-13.22	-13.16	-6.56	-8.93	-11.36	-2.99	-8.78	-10.19
17	11078	-13.33	-14.12	-12.63	-6.80	-9.98	-11.09	-3.09	-9.63	-10.07
18	11437	-13.78	-15.24	-12.18	-7.02	-11.10	-10.85	-3.18	-10.48	-9.96
19	11766	-14.19	-16.58	-11.75	-7.22	-12.23	-10.62	-3.26	-11.32	-9.86
20	12066	-14.56	-18.03	-11.35	-7.41	-13.33	-10.41	-3.33	-12.12	-9.76
21	12337	-14.90	-19.46	-10.90	-7.58	-14.35	-10.22	-3.40	-12.89	-9.68
22	12578	-15.20	-20.77	-10.67	-7.73	-15.28	-10.06	-3.47	-13.61	-9.68
23	12789	-15.47	-21.94	-10.39	-7.87	-16.13	-9.91	-3.52	-14.28	-9.53
24	12970	-15.70	-22.97	-10.15	-7.98	-16.90	-9.78	-3.56	-14.90	-9.46
25	13122	-15.89	-23.88	-9.94	-8.07	-17.59	-9.66	-3.60	-15.48	-9.41
26	13245	-16.04	-24.68	-9.77	-8.15	-18.22	-9.57	-3.63	-16.02	-9.36
27	13338	-16.15	-25.37	-9.64	-8.21	-18.79	-9.50	-3.65	-16.51	-9.32
28	13401	-16.23	-25.96	-9.55	-8.25	-19.29	-9.44	-3.67	-16.96	-9.29

Table VI. Calculated Activation Energies for the Halogens
from the Truncated Harmonic Oscillator Model II.

T RANGE	F ₂	Cl ₂	Br ₂	I ₂
200-400	37.1	56.9	45.2	35.1
400-600	36.8	56.6	44.7	34.5
600-800	36.2	56.2	44.1	33.9
800-1000	35.3	55.7	43.6	33.3
1000-1200	34.2	55.0	42.8	32.3
1200-1400	32.9	54.6	42.0	31.4
1400-1600	31.4	53.2	41.0	30.2
1600-1800	28.5	52.0	39.7	28.9
1800-2000	29.8	50.7	38.8	27.9
2000-2200	29.5	49.5	37.4	26.5
2200-2400	29.5	48.2	36.1	26.2
2400-2600	29.7	46.6	35.3	26.0
2600-2800	27.3	45.7	35.3	25.4
2800-3000	30.5	45.0	33.4	26.3

Table VII. Calculated Activation Energies for O_2 and N_2 , Model II.

CALCULATED ACTIVATION ENERGIES

T RANGE	O_2	N_2
500-1000	117.9	225.1
1000-1500	117.3	224.5
1500-2000	115.0	224.5
2000-2500	114.4	222.5
2500-3000	110.4	222.5
3000-3500	108.8	219.8
3500-4000	103.3	219.6
4000-4500	101.2	209.5
4500-5000	98.3	213.7
5000-5500	93.5	208.9
5500-6000	94.3	205.5
6000-6500	91.6	204.3
6500-7000	93.7	197.3
7000-7500	91.5	197.3
7500-8000	95.8	189.1

Titles to Figures

- Fig. 1. Truncated Harmonic Oscillator Model for Decomposition of Diatomic Molecule. For model I all c 's are assumed to be zero except c_t . For model II all c_i are allowed to be non-zero, Eq.(30). In each model only nearest neighbor transitions are considered for vibrational energy transfer.
- Fig. 2. Morse Function Model for Decomposition of Diatomic Molecule. Model III considers only nearest neighbor vibrational transfers, and model IV considers all vibrational energy transfers. Both models allow all states to dissociate to the continuum, Eq.(30).
- Fig. 3. Vibrational relaxation constant P_{10} for H_2 calculated as a function of temperature according to ref. 50 and the two observed constants as reported in ref. 47.
- Fig. 4. Dissociation of H_2 by Ar. Calculated and observed rate constants as a function of temperature.
- I. Calculated on the basis of the truncated harmonic oscillator, ladder-climbing model.
- IV. Calculated on the basis of the Morse function with all transitions allowed (compare Fig.3 and Table III).
- Observed functions as reported by reference 14
- a. ref. 39
 - b. ref. 40
 - c. ref. 41
 - d. ref. 42
 - e. ref. 43 where M is Xe (Ref. 41 reported Ar and Xe to have same efficiency in dissociating H_2).

Fig. 5. Distribution function for molecules that react for the vibrational states of F_2 with the Morse model IV, allowing all possible transitions (Fig. 3).

Note the shrinking number of states that contribute to reaction as one goes to high temperatures.

Fig. 6. Dissociation of Fluorine. Calculated curves: II. Truncated Harmonic Oscillator with all states allowed to dissociate to the continuum, Fig.2. IV. Full Morse function, Fig.3.

Observed data: \circ , with Ar, ref.15, points taken from graph; \bullet , with N_e , ref.16; \square , with N_e , ref.54, points taken from graph.

Fig. 7. Dissociation of Homonuclear Diatomic Molecules.

Calculated curves are based on model II, truncated harmonic oscillator, all transitions to continuum allowed (compare Fig.2). The lower curve is based on steady-state, non-equilibrium distribution function. The upper curve is based on the same model with the equilibrium distribution over vibrational states.

Experimental points are taken from tables or read from graphs in the articles cited. k in units of cc/particle -sec.

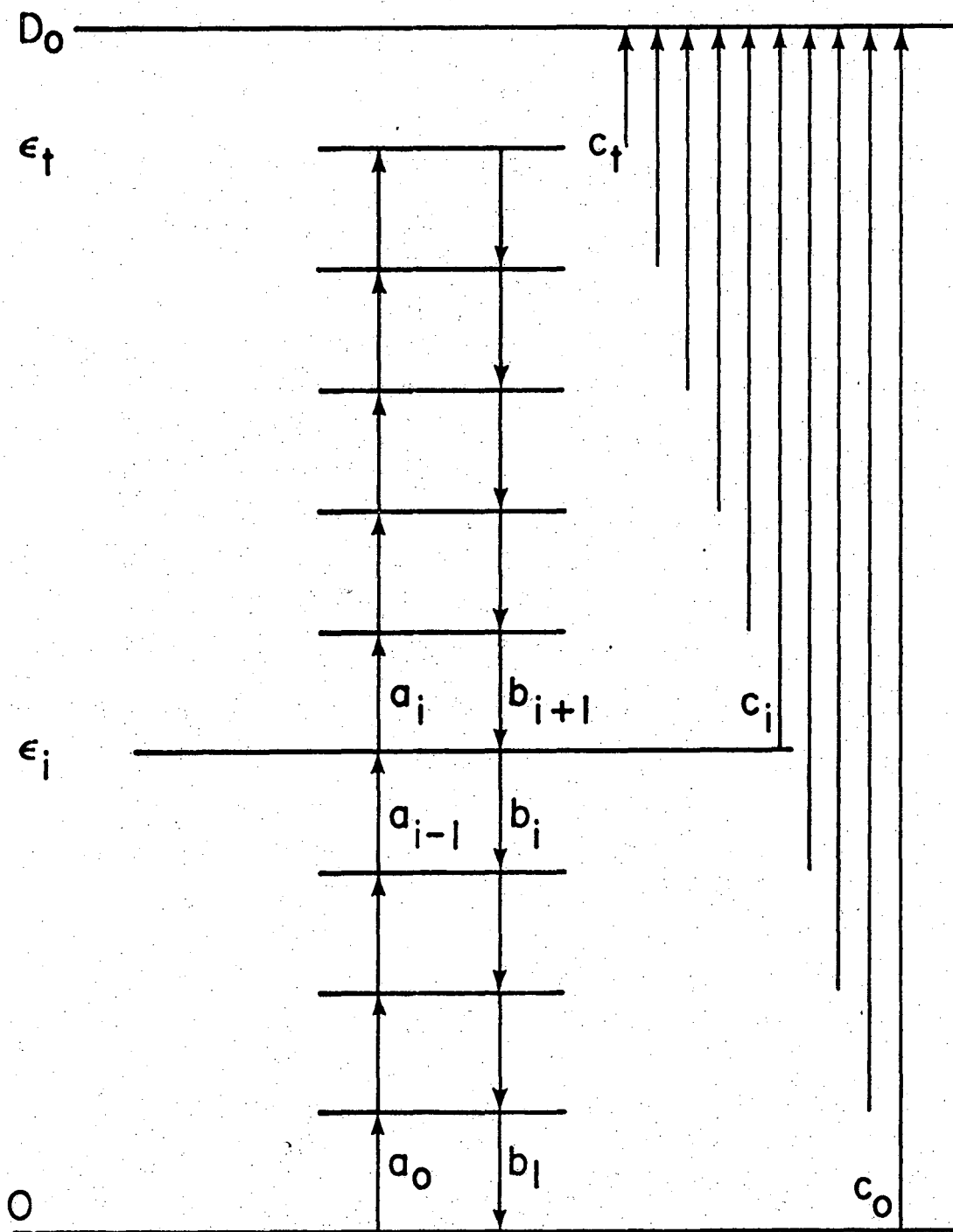
A. I_2 . \circ , with Ar, ref.26, read from graph; \bullet , with Ar, ref.27, read from graph (an error of a factor of 10 appears in the graph of ref.27, and this has been corrected).

B. Br_2 . \square , with Ar, ref.25; \blacksquare , Br_2 is M, ref.25; \blacklozenge , with Ar, ref.19; \blacklozenge , with Ar, ref.55; \bullet , with Ar, ref.56.

C. Cl_2 . \square , with Ar, ref.19; \circ , with Ar, ref.18; \bullet , with Ar, ref.20; \blacksquare , 5% Cl_2 in Ar, \blacklozenge , 10% Cl_2 in Ar, ref.21; \diamond , with Ar, ref.22.

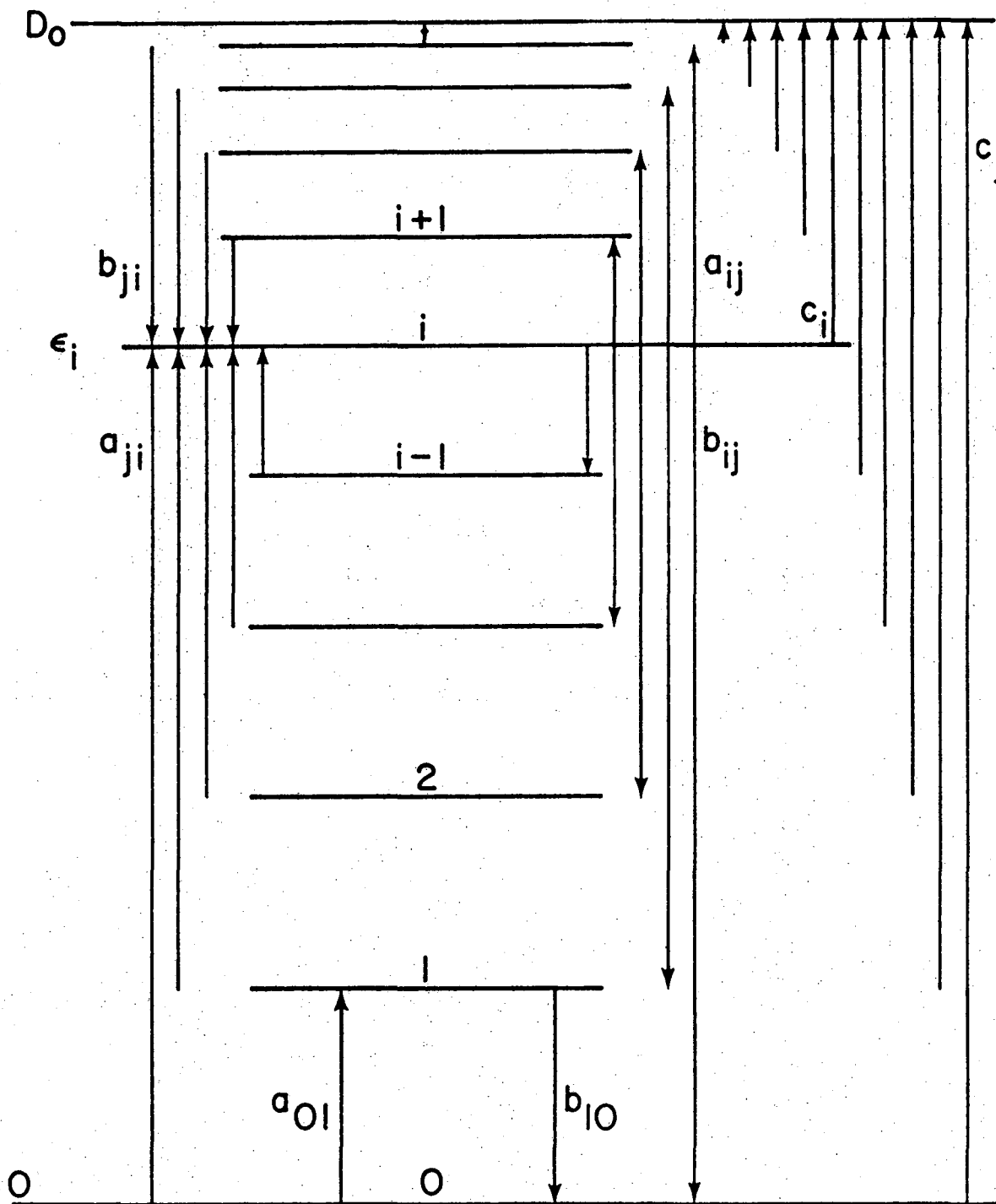
D. N_2 . \bullet , with Ar, ref.57, points read from graph.

E. O_2 . All data in excess Ar. Points as read from graphs listed in ref.29. \blacksquare , ref.34; \circ , ref.30; \diamond , ref.108 in ref.29; \bullet , ref.33.



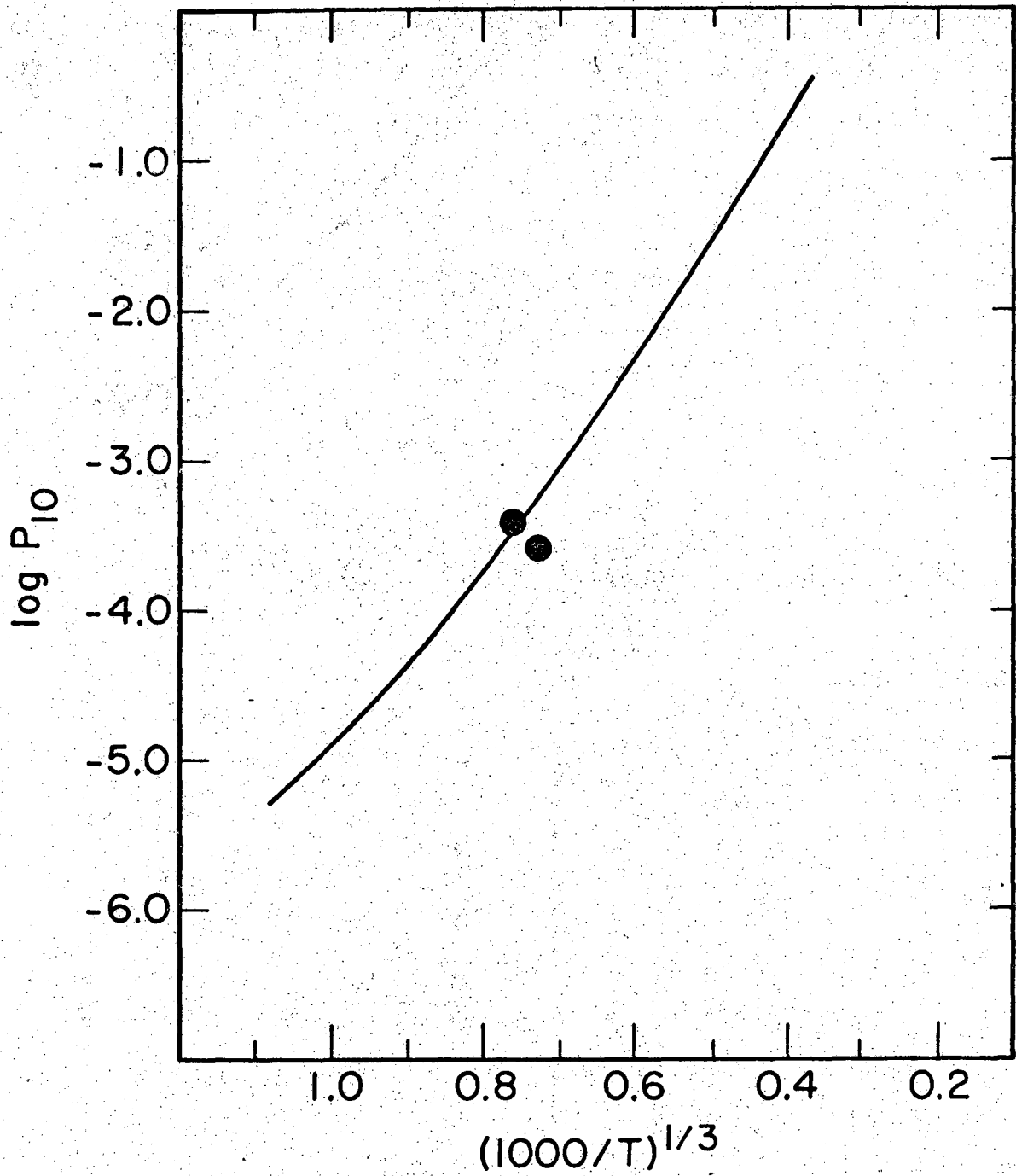
XBL 711-6423

Fig. 1



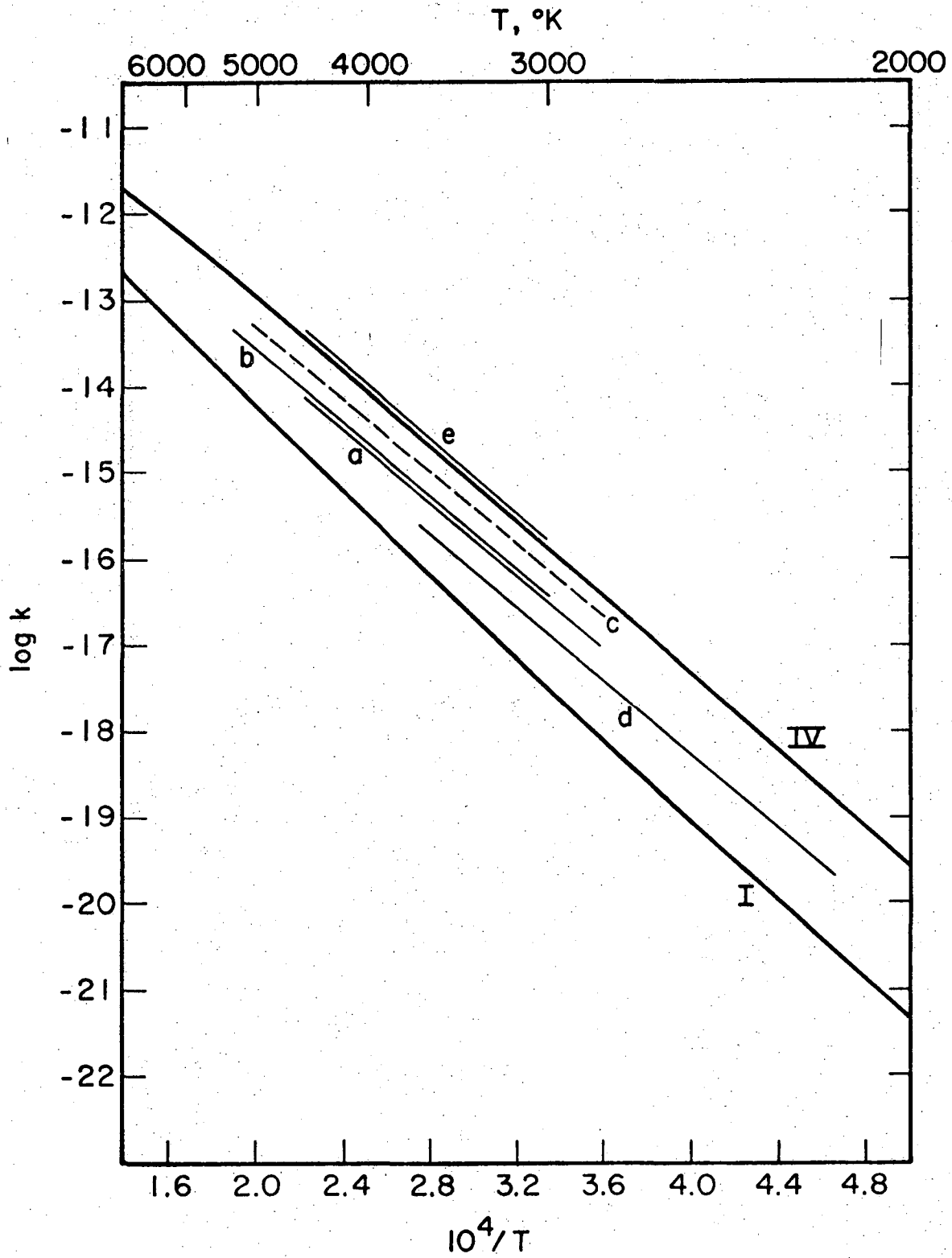
XBL 711-6424

Fig. 2



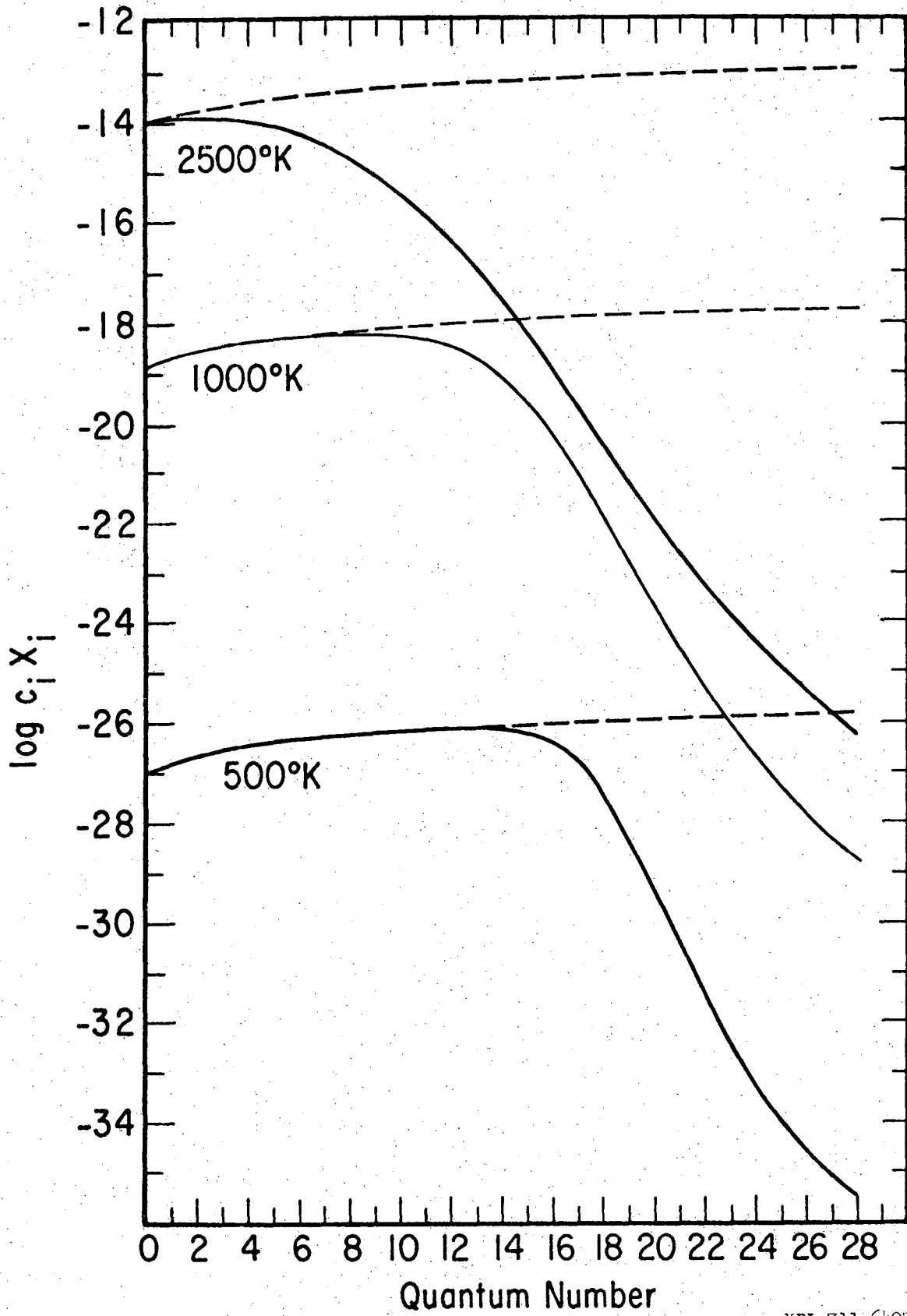
XBL 711-6425

Fig. 3



XBL 711-6426

Fig. 4



XBL 711-6427

Fig. 5

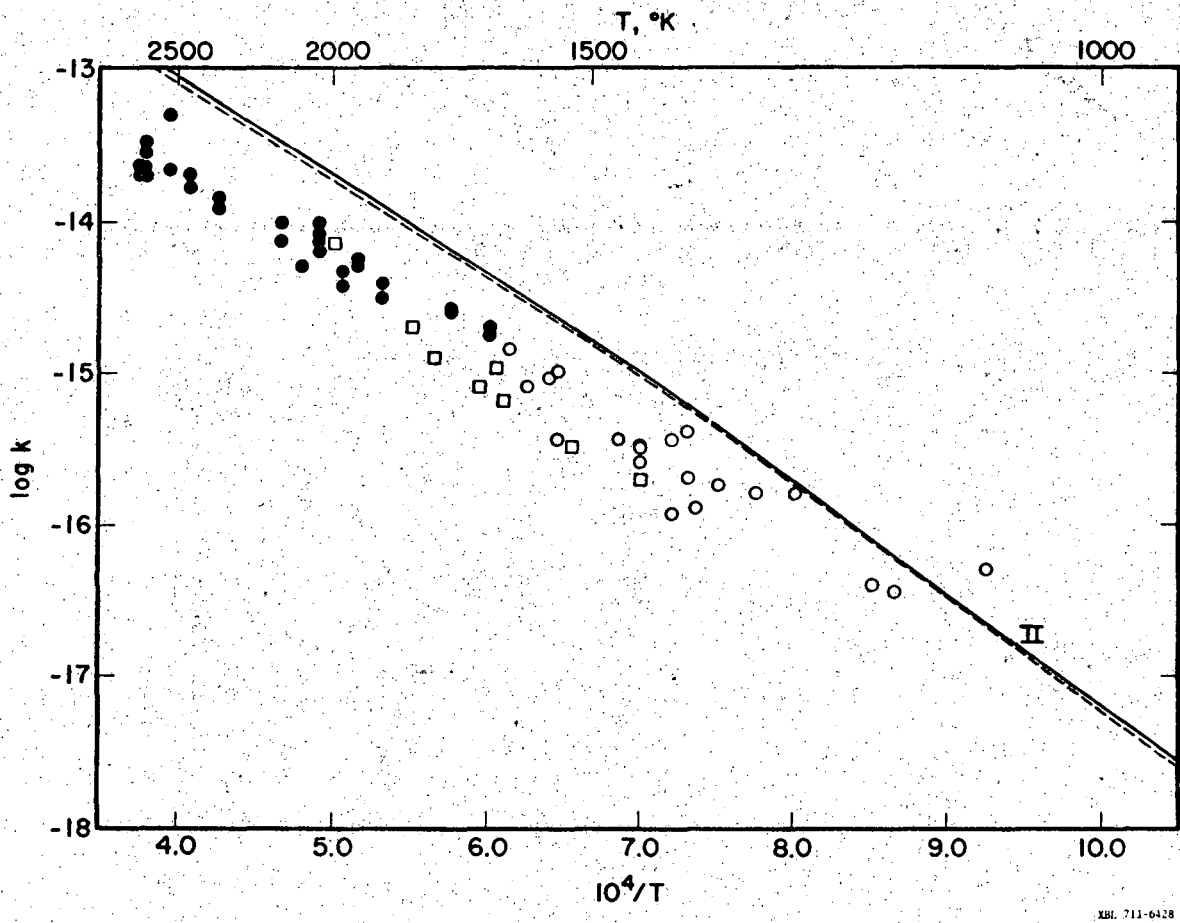
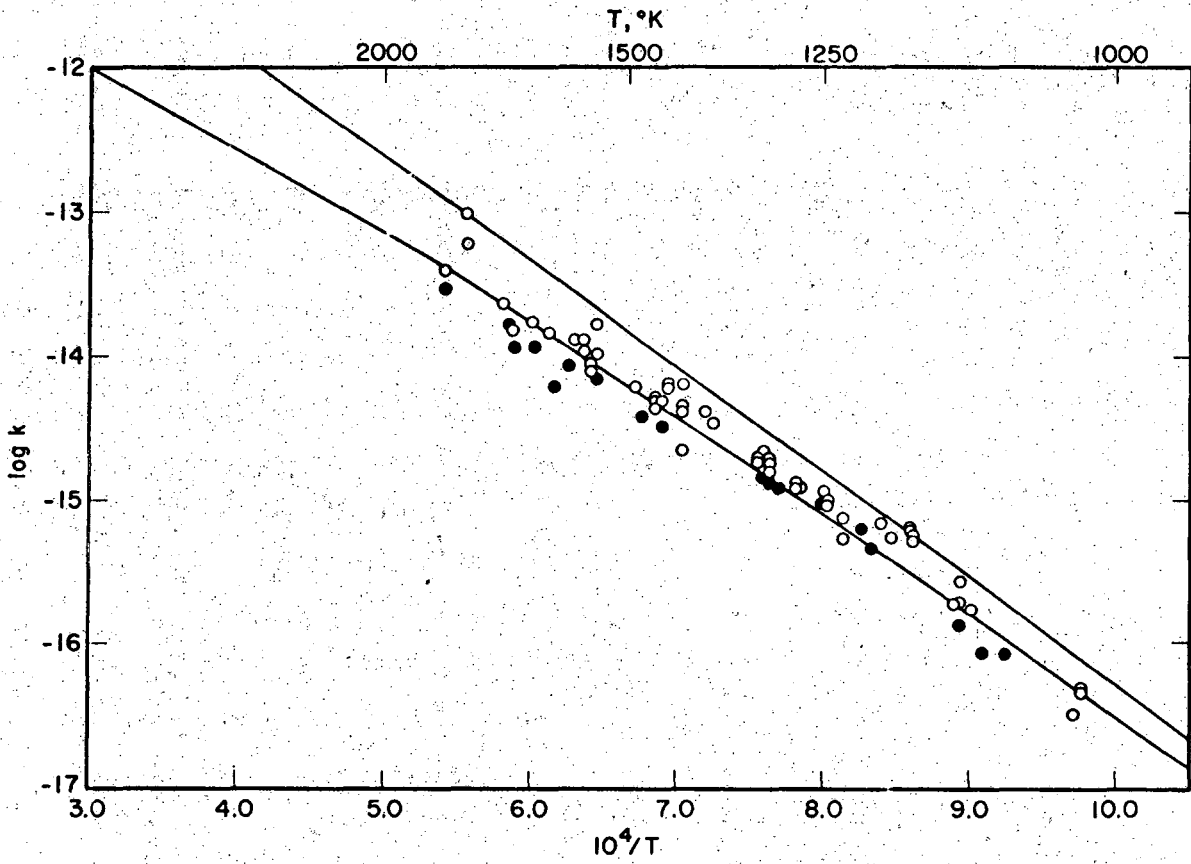


Fig. 6



NRL 711-6429

Fig. 7A.

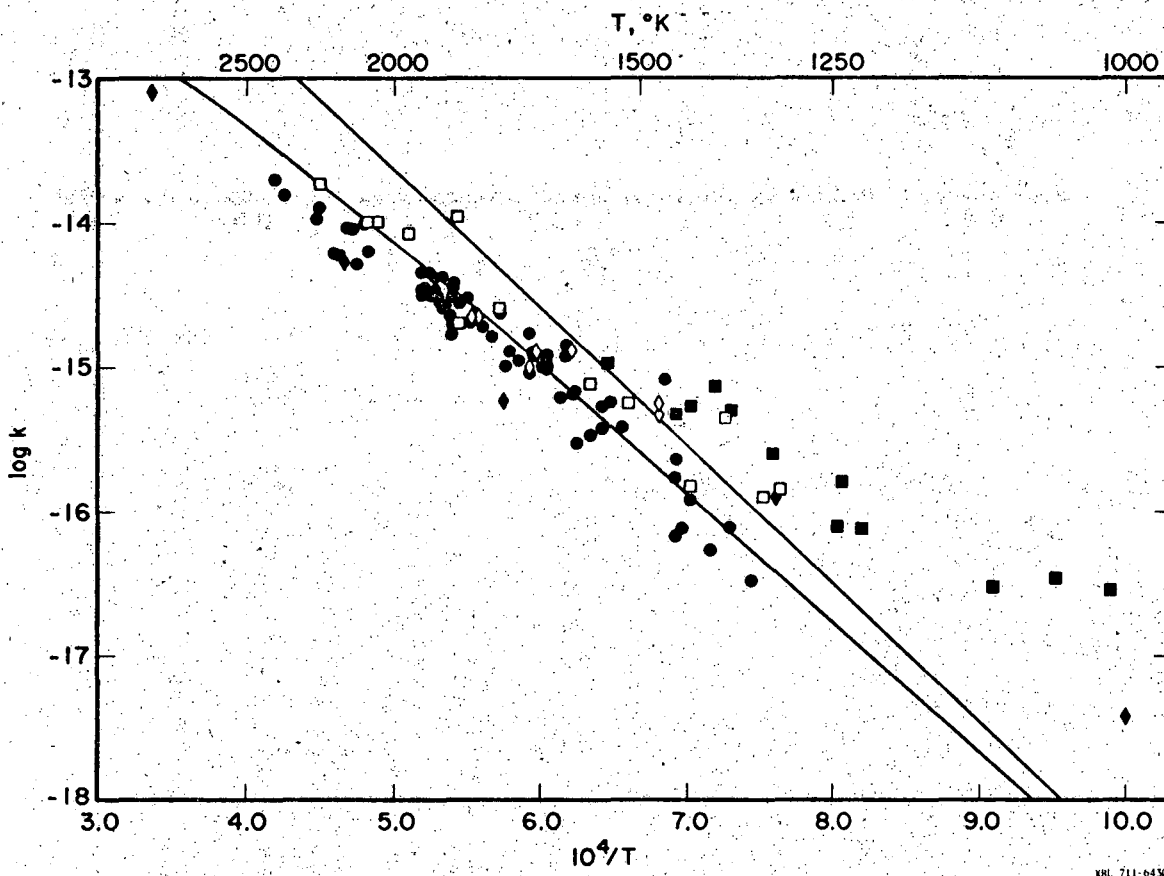


Fig. 7B.

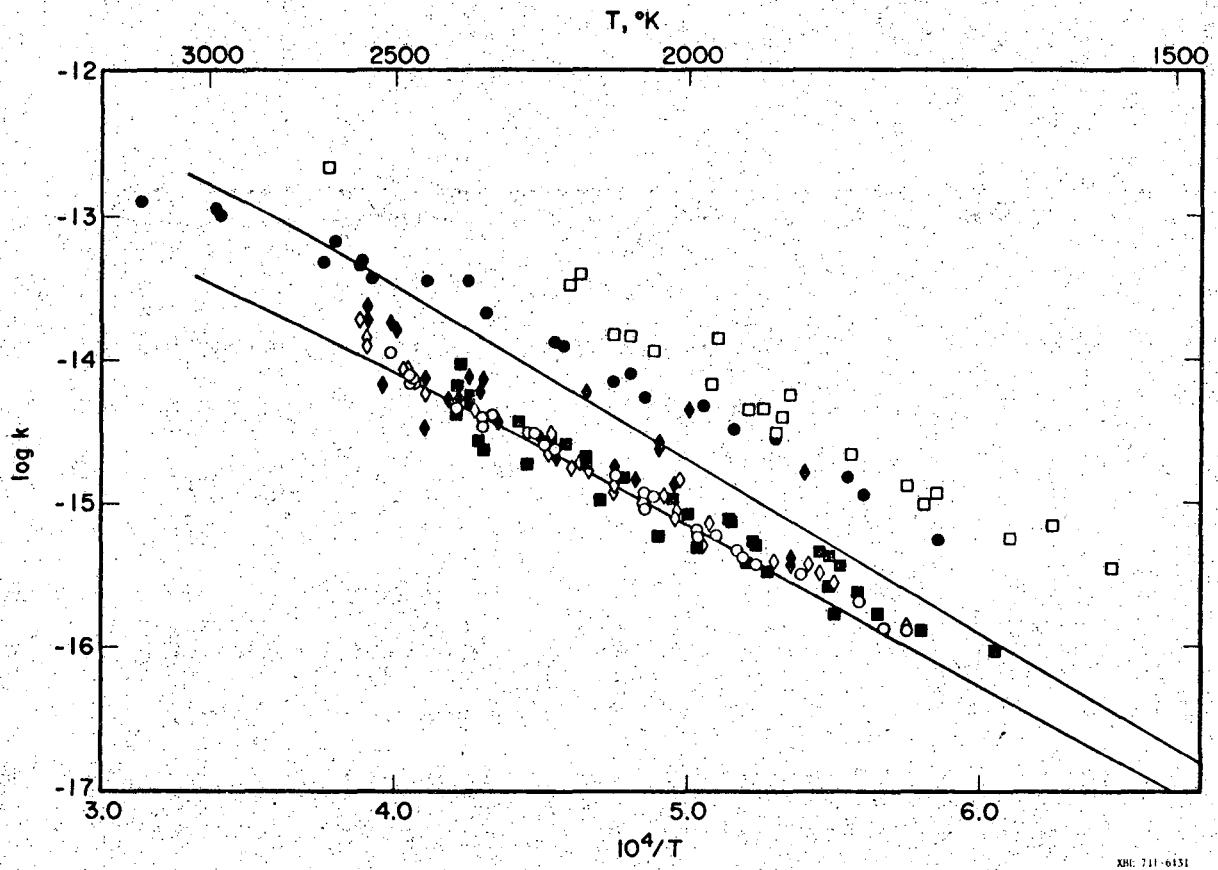
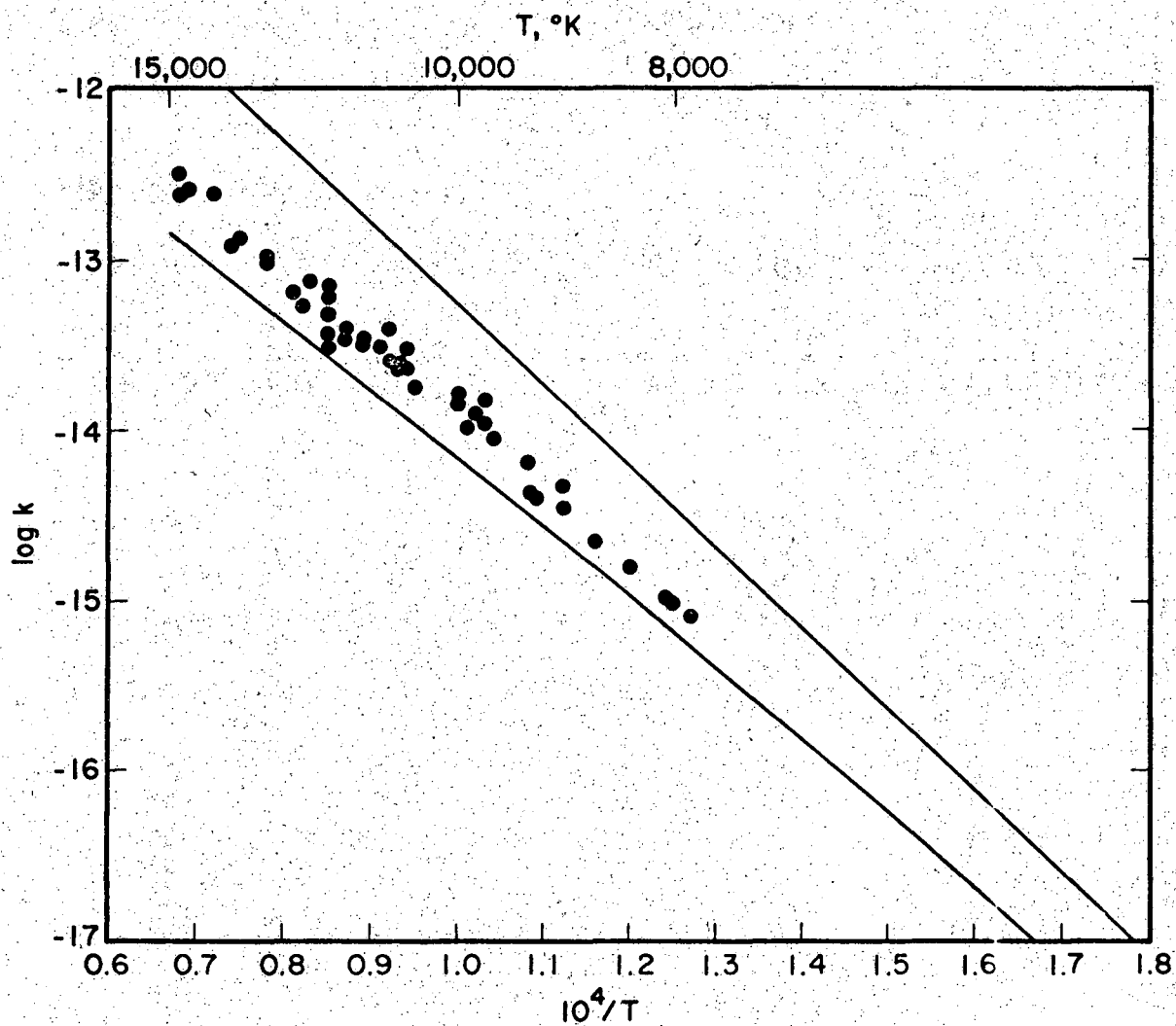
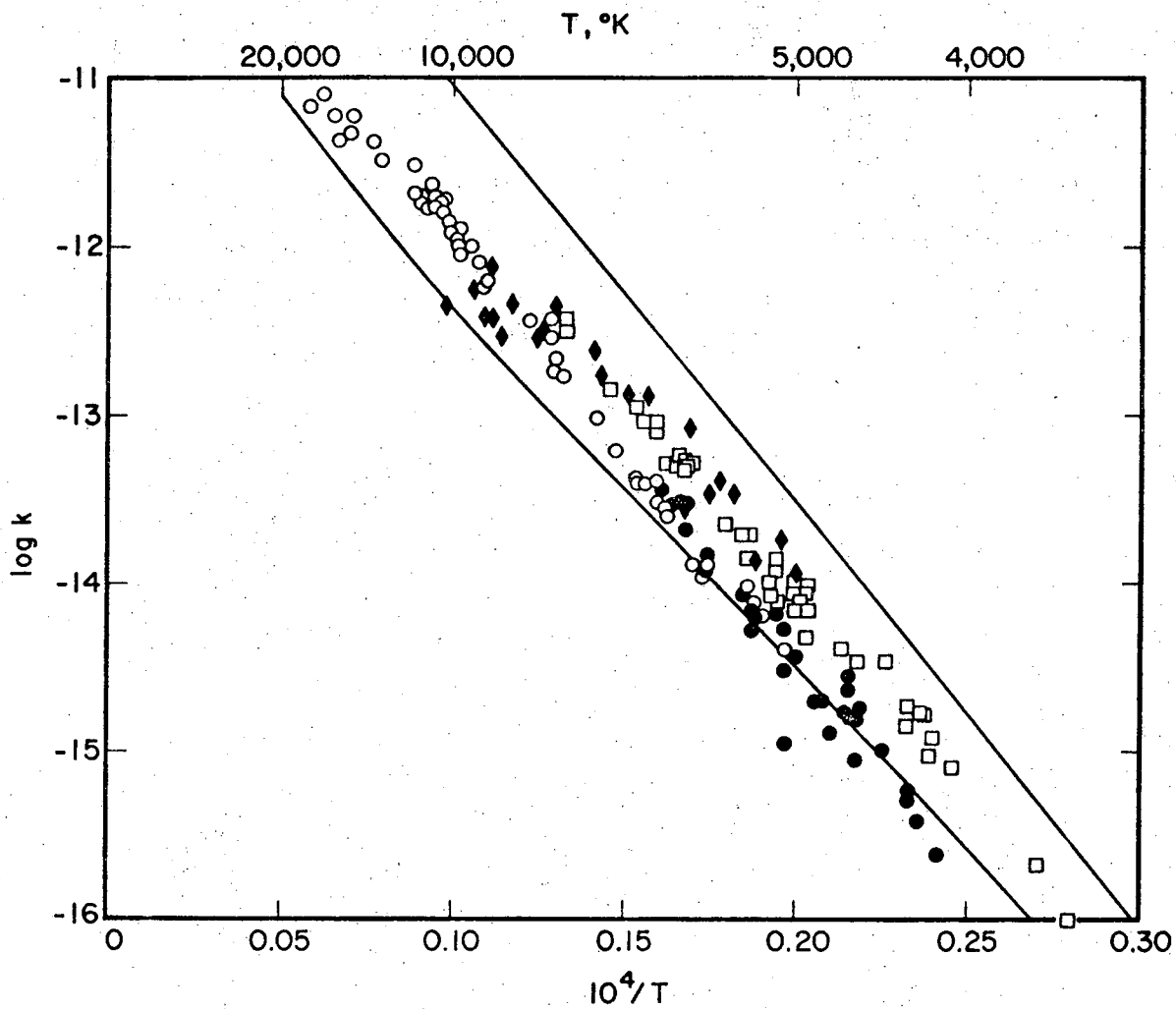


Fig. 7C.



XBL 711-6432

Fig. 7D.



XBL 711-6433

Fig. 7E.

LEGAL NOTICE

This report was prepared as an account of work sponsored by the United States Government. Neither the United States nor the United States Atomic Energy Commission, nor any of their employees, nor any of their contractors, subcontractors, or their employees, makes any warranty, express or implied, or assumes any legal liability or responsibility for the accuracy, completeness or usefulness of any information, apparatus, product or process disclosed, or represents that its use would not infringe privately owned rights.

TECHNICAL INFORMATION DIVISION
LAWRENCE RADIATION LABORATORY
UNIVERSITY OF CALIFORNIA
BERKELEY, CALIFORNIA 94720